J. Korean Wood Sci. Technol. 2019, 47(4): 442~450 pISSN: 1017-0715 eISSN: 2233-7180
https://doi.org/10.5658/WOOD.2019.47.4.442

Original Article

Pyrolysis of Lignin Obtained from *Cinnamyl Alcohol Dehydrogenase* (*CAD*) Downregulated *Arabidopsis Thaliana*[1]

Kwang Ho Kim[2,3] · Jae-Young Kim[4] · Chang Soo Kim[2] · Joon Weon Choi[4,†]

ABSTRACT

Despite its potential as a renewable source for fuels and chemicals, lignin valorization still faces technical challenges in many aspects. Overcoming such challenges associated with the chemical recalcitrance of lignin can provide many opportunities to innovate existing and emerging biorefineries. In this work, we leveraged a biomass genetic engineering technology to produce phenolic aldehyde-rich lignin structure via downregulation of *cinnamyl alcohol dehydrogenase (CAD)*. The structurally altered lignin obtained from the *Arabidopsis thaliana CAD* mutant was pyrolyzed to understand the effect of structural alteration on thermal behavior of lignin. The pyrolysis was conducted at 400 and 500 °C using an analytical pyrolyzer connected with GC/MS and the products were systematically analyzed. The results indicate that aldehyde-rich lignin undergoes fragmentation reaction during pyrolysis forming a considerable amount of C6 units. Also, it was speculated that highly reactive phenolic aldehydes facilitate secondary repolymerization reaction as described by the lower yield of overall phenolic compounds compared to wild type (WT) lignin. Quantum mechanical calculation clearly shows the higher electrophilicity of transgenic lignin than that of WT, which could promote both fragmentation and recondensation reactions. This work provides mechanistic insights toward biomass genetic engineering and its application to the pyrolysis allowing to establish sustainable biorefinery in the future.

Keywords: cinnamyl alcohol dehydrogenase, lignin, pyrolysis, densify functional theory, electrophilicity

1. INTRODUCTION

Lignin, one of the primary biomass components along with cellulose and hemicellulose, accounts 15 − 30 % by weight of the lignocellulosic biomass (Yang and Pan, 2016). In addition to the existing pulp and paper industries, a massive amount of lignin is expected to be collected from the emerging lignocellulosic biorefineries (Kim and Kim, 2018). From the techno-economic standpoint, lignin valorization holds the key to success in the future biorefinery (Ragauskas *et al.*, 2014). Despite the potential promise of lignin utilization, lignin is still poorly utilized due to its inherent recalcitrance.

There have been enormous efforts to overcome the technical barriers associated with lignin. In this regard, plant genetic engineering to alter lignin content and/or composition in the biomass cell wall structure has been

[1] Date Received March 25, 2019, Date Accepted July 8, 2019
[2] Clean Energy Research Center, Korea Institute of Science and Technology, Seoul, 02792, Republic of Korea
[3] Department of Wood Science, University of British Columbia, Vancouver, BC, V6T 1Z4, Canada
[4] Graduate School of International Agricultural Technology and Institute of Green-Bio Science and Technology, Seoul National University, Pyeongchang, 25354, Republic of Korea
[†] Corresponding author: Joon Weon Choi (e-mail: cjw@snu.ac.kr, ORCID: 0000-0002-9454-0475)

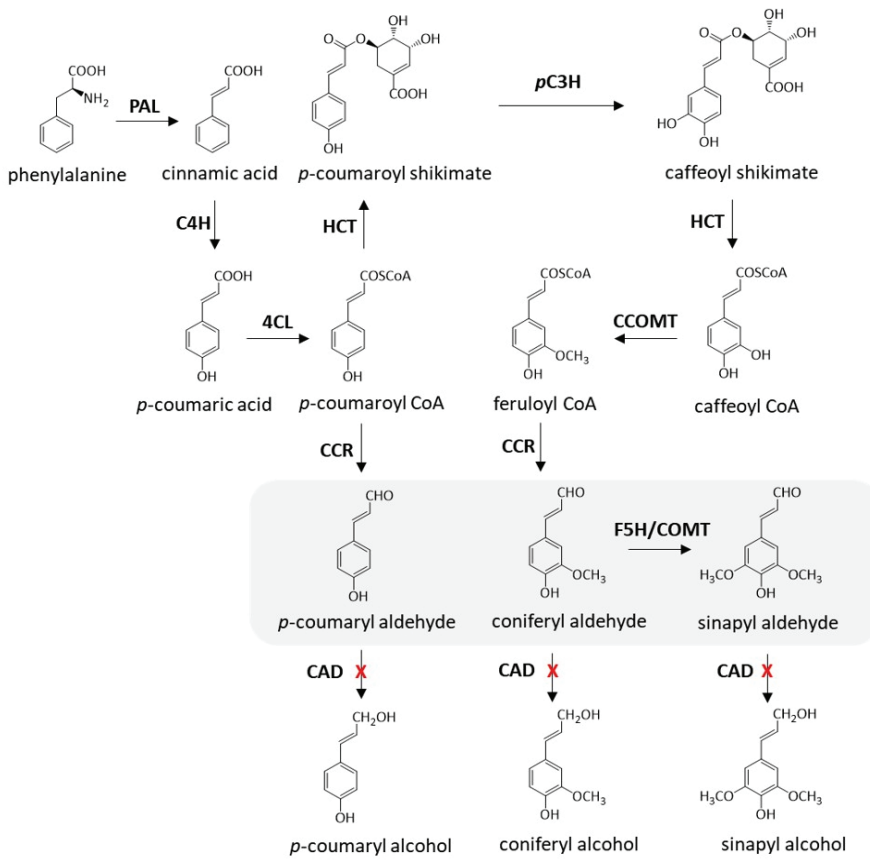

Fig. 1. The main pathway involved in monolignol biosynthesis in biomass cell wall. The three monolignol precursors shown with a gray background resulted from the downregulation of *CAD* gene. *PAL*, phenylalanine ammonia lyase; *C4H*, cinnamate 4-hydroxylase; *4CL*, 4-coumaric acid-CoA ligase; *HCT*, hydroxycinnamoyl-CoA shikimate hydroxycinnamoyl transferase; *pC3H*, *p*-coumarate 3-hydroxylase; *CCR*, cinnamoyl-CoA reductase; *CCOMT*, caffeoyl-CoA *O*-methyltransferase; *F5H*, ferulate 5-hydroxylase; *COMT*, caffeic acid *O*-methyltransferase; *CAD*, cinnamyl alcohol dehydrogenase.

widely studied (Mahon and Mansfield, 2019). As shown in Fig. 1, there are many enzymes participate in the phenylpropanoid pathway, many of them have been considerably examined. For example, studies reported that manipulating monolignol biosynthesis genes such as cinnamate 4-hydroxylase (*C4H*), cinnamoyl-CoA reductase (*CCR*), caffeic acid O-methyltransferase (*COMT*) and cinnamyl alcohol dehydrogenase (*CAD*) can produce biomass with structurally altered lignin. Strategic downregulation of *CAD* gene during the lignin monolignol biosynthesis pathway accumulates more *p*-coumaryl aldehyde, coniferyl aldehyde and sinapyl aldehyde. These three phenolic aldehyde precursors participate in lignin biosynthesis in the plant cell wall forming unique interunit linkages as shown in Fig. 2 (Zhao *et al.*, 2013).

Fast pyrolysis of lignin has gained enormous attention as it can produce valuable phenol and phenolics (Kim, *et al.* 2011, Kim, *et al.*, 2015a). However, reactions behind lignin pyrolysis are extremely complex and can

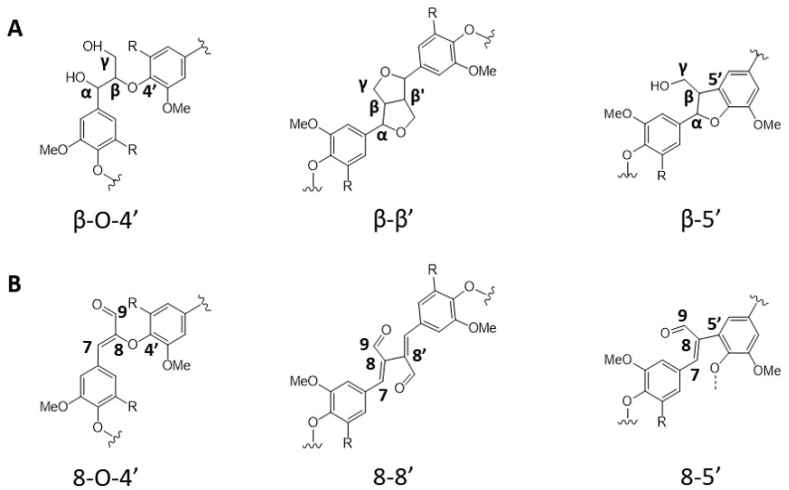

Fig. 2. (A) Main structures of typical lignin subunits and (B) new structures present in the lignin of *CAD* downregulated biomass (Zhao *et al*., 2013).

be influenced by many factors including source, purity and interunit linkages of lignin. Although the pyrolysis of lignin has been studied over the past decades, only a few studies focused on the effect of genetic alteration of lignin on pyrolysis.

In this work, lignin samples extracted from WT and *CAD* downregulated biomass are pyrolyzed using an analytical pyrolyzer to understand how the strategic alteration of lignin composition affects the products yield and distributions. Also, we report the results of a computational study investigating the chemical reactivity of engineered lignin structure. This work could provide insights toward developing a biomass processing integrated with plant genetic engineering and thermochemical conversion technology.

2. MATERIALS and METHODS

2.1. Materials

Arabidopsis thaliana seeds from wildtype (WT) and *CAD* double mutant (*cad-c* and *cad-d*) were germinated directly on the soil. The details, including gene identification, plant growth and other analyses, have been previously described (Sibout *et al.*, 2005). Lignin was extracted from both WT and *CAD* mutant biomass for pyrolysis test. Each biomass sample was finely ground and subjected to enzymatic hydrolysis, followed by mild acidolysis to extract pure lignin (Guerra *et al.*, 2008). Physicochemical properties of both WT and *CAD* mutant lignin, including molecular weight and 2D HSQC NMR spectra for interunit linkage analysis, are well described in the literature (Kim *et al.*, 2019).

2.2. Fast pyrolysis

A coil-type CDS Pyroprobe 5000 (CDS Analytical Inc., Oxford, PA, USA) was used in this study. In sample preparation, 0.7-0.8 mg of lignin was introduced to a quartz tube with 1.25 μL internal standard (IS; 3.9 mg of fluoranthene/mL of methanol) for quantification of pyrolysis products (Kim *et al.*, 2013, Kim *et al.*, 2015b). The sample was pyrolyzed at 400 and 500 °C with a heating rate of 10 °C/ms and maintained for 20 s at a final temperature in an inert atmosphere. During pyrolysis, the pyrolyzer interface and transfer line were

maintained at 250 °C. The released pyrolysis products were on-line transferred to a GC-MS/FID instrument (Agilent Technologies 7890A/Agilent Technologies 5975A, USA) equipped with a DB-5 capillary column (30 m×0.25 mm ID×0.25 μm film thickness) with a split ratio of 1:100. The separated products were split equally to FID and MS system. The gas chromatograph injector and detector temperature were set at 250 °C and 300 °C, respectively. The oven temperature began at 50 °C for 5 min and then up to 280 °C with a heating rate of 3 °C/min. It maintained for 10 min at final temperature.

The MS source temperature and MS quad temperature was 230 °C and 150 °C, respectively. The separated products were introduced into the ionization source of a quadrupole MS. The ionization was achieved with electron impact (EI) mode at 70 eV. The mass spectrometer was scanned from m/z=50 to m/z = 550. Identification of each compound was based on the NIST MS Search 2.0 (NIST/EPA/NIH Mass Spectral Library; NIST 02) and proper reference (Faix *et al.*, 1990). For quantitative analysis, the response factor (RF) between each authentic compound and the IS was determined by GC-FID information (Kim *et al.*, 2015a).

2.3. Computational analysis

Computational study was conducted to understand the chemical reactivity of WT and *CAD* mutant lignin. First, the geometry optimization of the typical β-O-4' dimeric model compound found in WT (guaiacylglycerol-β-guaiacyl ether) and 8-O-4' dimer in *CAD* mutant (guaiacylacrylaldehyde-β-guaiacyl ether) was carried out using density functional theory (DFT) with the B3LYP functional and the 6-31+G(d,p) basis set (Shi *et al.*, 2016). Frequency calculation was conducted to verify that the optimized structures corresponded to energy minima. Herein, the DFT-based global electrophilicity index (ω, eV) was calculated using Gaussian 09 software (Socha *et al.*, 2014). Equations for the calculation of the electronegativity (χ, eV) and the hardness (η, eV) is given as

$$\chi\,(eV) = -\frac{E_{HOMO} + E_{LUMO}}{2} \quad \cdots\cdots (1)$$

$$\eta\,(eV) = \frac{E_{LUMO} - E_{HOMO}}{2} \quad \cdots\cdots (2)$$

where E_{HOMO} and E_{LUMO} are the energies of the highest occupied and lowest unoccupied molecular orbitals, respectively. The electrophilicity index is defined as (Chattaraj *et al.*, 2006)

$$\omega\,(eV) = \frac{\chi^2}{2\eta} \quad \cdots\cdots (3)$$

3. RESULTS and DISCUSSION

3.1. Fast pyrolysis

Fast pyrolysis of WT and *CAD* mutant samples was conducted at 400 and 500 °C (Fig. 3). Table 1 shows the list of compounds analyzed from the pyrolysis runs. As presented, 22 lignin derivatives were identified and quantified. The total amount of lignin derivatives from the pyrolysis of WT was 57.3 and 91.8 μg/mg lignin at 400 and 500 °C, respectively. Among the compounds analyzed, guaiacol, creosol, eugenol, 4-vinylguaiacol and isoeugenol were the major products from WT. In *CAD* mutant lignin, the distribution of the pyrolysis products was different from WT and the total amount of the products was about 56.3 μg/mg lignin at 500 °C, which is 38.7% lower than WT. Syringol, guaiacol, *p*-cresol, toluene and creosol were the main products from the pyrolysis of *CAD* mutant. Interestingly, aromatic hydrocarbons including toluene, ethylbenzene and styrene were produced from the pyrolysis of *CAD* mutant whereas the yields of those from the WT were insignificant. The pyrolysis products were further

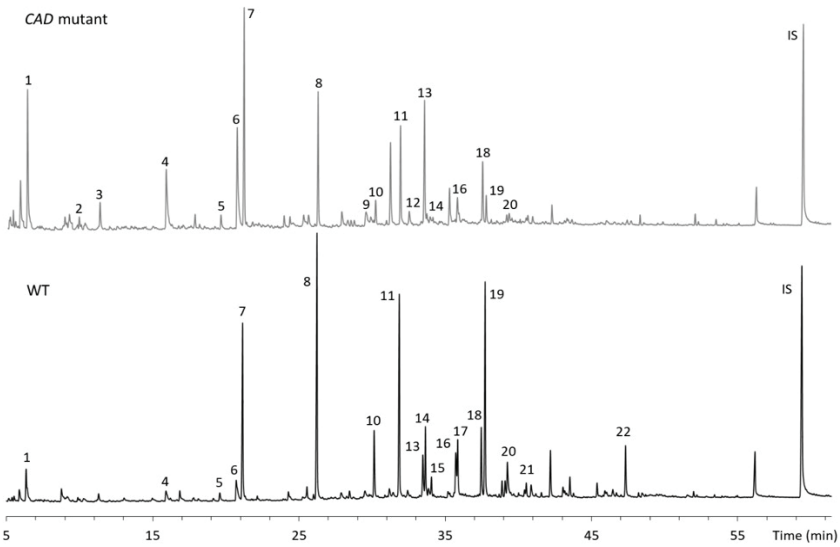

Fig. 3. Gas chromatograms obtained from the pyrolysis of WT and *CAD* mutant at 500 °C.

Table 1. The yield of pyrolysis products from WT and *CAD* mutant lignin at 400 and 500 °C (μg/mg lignin).

	Compound	500 °C		400 °C	
		WT	CAD mutant	WT	CAD mutant
1	Toluene (AH)	2.20 ± 0.17	6.45 ± 0.17	0.58 ± 0.14	2.21 ± 0.03
2	Ethylbenzene (AH)	n.d.	0.37 ± 0.05	n.d.	n.d.
3	Styrene (AH)	n.d.	1.36 ± 0.05	n.d.	n.d.
4	Phenol (C6; H)	0.91 ± 0.09	4.38 ± 0.16	n.d.	2.59 ± 0.26
5	*o*-Cresol (C1C6; H)	0.51 ± 0.06	0.70 ± 0.01	n.d.	n.d.
6	*p*-Cresol (C1C6; H)	1.94 ± 0.16	6.38 ± 0.28	n.d.	2.73 ± 0.07
7	Guaiacol (C6; G)	7.84 ± 0.70	8.46 ± 0.17	4.06 ± 0.35	6.80 ± 0.28
8	Creosol (C1C6; G)	12.04 ± 0.71	4.96 ± 0.11	5.12 ± 0.59	2.85 ± 0.08
9	3-Methoxycatechol (C6; G)	n.d.	1.28 ± 0.17	n.d.	n.d.
10	4-Ethylguaiacol (C2C6; G)	2.42 ± 0.21	0.79 ± 0.01	0.71 ± 0.12	0.43 ± 0.03
11	4-Vinylguaiacol (C2C6; G)	6.37 ± 0.37	2.60 ± 0.03	6.30 ± 0.55	2.40 ± 0.16
12	3-Methoxy-5-methylphenol (C1C6; G)	n.d.	0.72 ± 0.17	n.d.	n.d.
13	Syringol (C6; S)	3.47 ± 0.18	8.34 ± 0.21	2.10 ± 0.08	7.61 ± 0.18
14	Eugenol (C3C6; G)	8.90 ± 0.36	1.37 ± 0.03	6.35 ± 0.73	1.43 ± 0.09
15	4-Propylguaiacol (C3C6; G)	0.69 ± 0.04	n.d.	n.d.	n.d.
16	Vanillin (C1C6; G)	1.58 ± 0.06	0.46 ± 0.07	1.03 ± 0.06	n.d.
17	*cis*-Isoeugenol (C3C6; G)	7.73 ± 0.33	n.d.	4.56 ± 0.83	n.d.
18	4-Methylsyringol (C1C6; S)	3.04 ± 0.16	2.68 ± 0.17	1.62 ± 0.19	1.82 ± 0.03
19	*trans*-Isoeugenol (C3C6; G)	28.39 ± 1.59	3.32 ± 0.05	24.08 ± 2.30	n.d.
20	Acetoguaiacone (C2C6; G)	1.22 ± 0.05	0.21 ± 0.02	0.78 ± 0.03	n.d.
21	Methyl vanillate (C3C6; G)	0.30 ± 0.07	n.d.	n.d.	n.d.
22	Methoxyeugenol (C3C6; S)	2.29 ± 0.05	n.d.	n.d.	n.d.
	Total	91.84 ± 5.36	56.33 ± 1.95	57.29 ± 5.97	31.31 ± 1.21

AH: aromatic hydrocarbon, H: p-hydroxyl phenyl units, G: guaiacyl units, S: syringyl units.

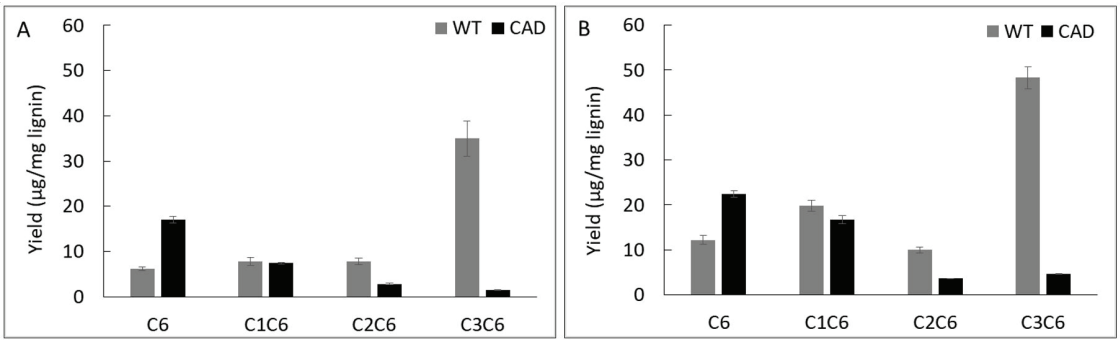

Fig. 4. Yields of lignin derivatives based on number of carbons in side chain obtained at 400 °C (left) and 500 °C (right).

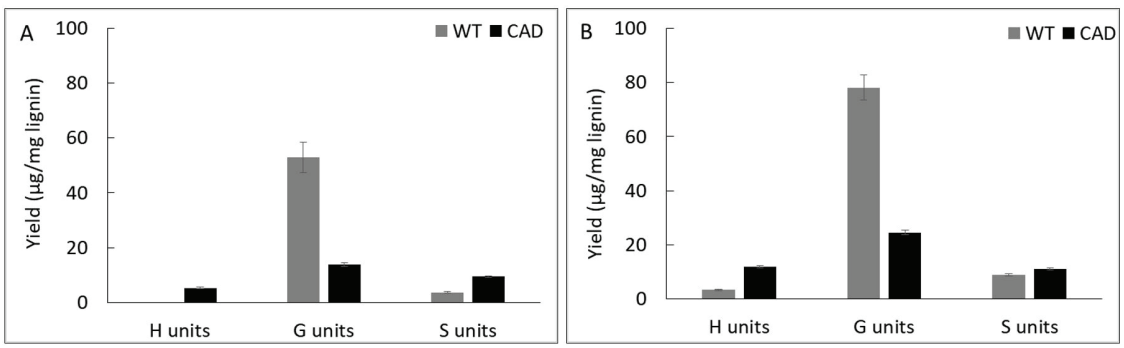

Fig. 5. Yields of lignin derivatives based on lignin subunits (H, G and S units) obtained at 400 °C (left) and 500 °C (right).

analyzed based on their substructure to understand how the thermal behavior of *CAD*-downregulated lignin is different from the WT lignin.

Fig. 4 shows the yield of pyrolysis products from lignins based on number of carbons in the side chain, namely C6, C1C6, C2C6 and C3C6. As shown in this figure, the yield of C6 units from *CAD* mutant was significantly higher that from WT. When pyrolyzed at 400 °C, the yield of C6 units from WT was 6.2 μg/mg lignin while that from *CAD* mutant was 17.0 μg/mg lignin. At 500 °C, the yield of C6 units from *CAD* transgenic further increased to 22.5 μg/mg lignin, which is almost a twofold compared to the WT. In contrast to the C6 products, the WT yielded higher yields of C1C6, C2C6 and C3C6 units at 400 and 500 °C. This implies that fragmentation of side chain in the lignin structure occurred significantly from the *CAD* mutant producing C6 product. Typically, thermal decomposition of lignin starts from the cleavage of aryl-ether linkage, the weakest bond in lignin structure, followed by a series of cleavage reactions. Apparently, the aldehyde-rich lignin from *CAD* mutant underwent secondary fragmentation reaction due to its reduced recalcitrance or increased reactivity.

The pyrolysis products were further categorized by their subunits according to the number of methoxyl group (Fig. 5). At 400 °C, guaiacyl (G) units account for the majority of the pyrolysis products followed by syringyl (S) and *p*-hydroxy phenyl (H) units from the WT and transgenic lignin. At 500 °C, the same trend

was observed from the WT whereas transgenic lignin yielded slightly higher H units (11.9 μg/mg lignin) than S units (11.0 μg/mg lignin) suggesting that defunctionalization reaction significantly occurred. This could be attributed to the increased reactivity of aldehyde-rich lignin structure upon pyrolysis at high temperature.

3.2. Computational modeling

As observed above, aldehyde-rich lignin structure resulted from the strategic downregulation of *CAD* gene shows increased fragmentation reaction, which is different from the thermal behavior of WT lignin. Thus, it is logically hypothesized that *CAD* downregulated lignin has high reactivity toward chemical and/or thermochemical reactions. To prove this hypothesis, the computational simulation was performed to understand the effect of *CAD* downregulation on the chemical reactivity of lignin. In this work, each representative dimeric model compound from WT (β-O-4') and *CAD* mutant (8-O-4') was used for the computational study. Considering the complex and heterogeneous structure of lignin, it is reasonable to employ the lignin model dimers with representative interunit linkages (aryl-ether). Fig. 6 illustrates the optimized geometry of two dimeric model compounds obtained from DFT based calculations. The electrophilicity index of two model dimers was calculated as a descriptor of reactivity that shows the global electrophilic nature of a molecule (Shi et al., 2016). As shown in Fig. 7, the electrophilicity index of a typical β-O-4' dimer is 1.78 eV while that of 8-O-4' dimer is 4.06 eV. Clearly, 8-O-4' structure has a higher electrophilicity index, indicating that *CAD* mutant lignin is chemically more reactive compared to the WT lignin (Carmona *et al.*, 2015). As observed from the pyrolysis, the relatively higher yield of fragmented products (i.e., C6 units) from *CAD* mutant is likely attributed to its reactive structure. Additionally, it should be noted that the higher reactivity of *CAD*

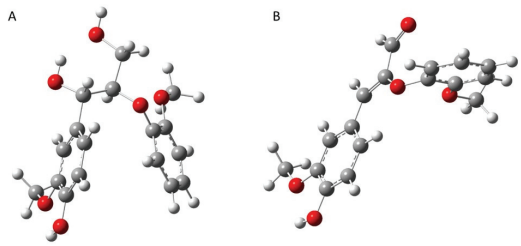

Fig. 6. Optimized geometry of (A) β-O-4' (guaiacylglycerol-β-guaiacyl ether) structure found in WT and (B) 8-O-4' dimer (guaiacylacrylaldehyde-β-guaiacyl ether) found in *CAD* downregulated biomass.

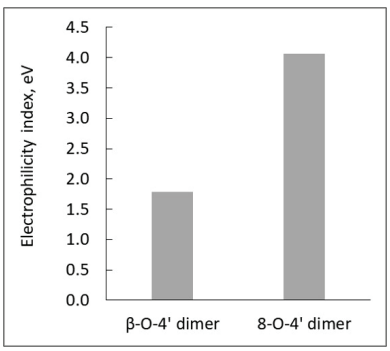

Fig. 7. Electrophilicity index of β-O-4' structure found in WT and 8-O-4' dimer found in *CAD* downregulated biomass.

mutant lignin could facilitate repolymerization and charring reaction. Aldehydes are reactive functional groups and typically responsible for repolymerization reaction during the depolymerization of lignin (Kim *et al.*, 2015c). The lower yield of pyrolysis products from *CAD* mutant than WT is possibly associated with a highly reactive characteristic of aldehyde-rich lignin. Overall, the product distribution along with computational simulation indicate the occurrence of two competing reaction pathways, which are fragmentation and repolymerization reactions. Although more in-depth analyses are necessary to elucidate the reaction mechanisms, the results clearly support the hypothesis that *CAD* downregulation changes the thermal behavior and product distribution of lignin.

4. CONCLUSION

Plant genetic engineering has been widely used to overcome biomass recalcitrance. In this work, pyrolysis of lignins obtained from WT and *CAD* downregulated Arabidopsis was conducted to understand the effect of *CAD* downregulation on products distribution. The results suggest that *CAD* transgenic biomass undergoes relatively more fragmentation and repolymerization reaction compare to the WT. The highly reactive aldehyde-rich structure of *CAD* mutant, described by higher electrophilicity index calculated by computational analysis, clearly support the hypothesis. This result provides mechanistic insights toward biomass genetic engineering and its application to the thermal depolymerization. Finally, integrative and interdisciplinary research will provide the basis for establishing sustainable biorefinery in the future.

ACKNOWLEDGMENT

This work was supported by the Korea Institute of Science and Technology (KIST) − University of British Columbia (UBC) Biorefinery On-site Laboratory program. Authors would like to thank Aymerick Eudes at Joint BioEnergy Institute for generously providing the wild type and transgenic *Arabidopsis* samples.

REFERENCES

Carmona, C., Langan, P., Smith, J.C., Petridis, L. 2015. Why genetic modification of lignin leads to low-recalcitrance biomass. Physical Chemistry Chemical Physics 17(1): 358-364.

Chattaraj, P.K., Sarkar, U., Roy, D.R. 2006. Electrophilicity index. Chemical Reviews 106(6): 2065-2091.

Faix, O., Meier, D., Fortmann, I. 1990. Thermal degradation products of wood. European Journal of Wood and Wood Products 48(7): 281-285.

Guerra, A., Lucia, L.A., Argyropoulos, D.S. 2008. Isolation and characterization of lignins from Eucalyptus grandis Hill ex Maiden and Eucalyptus globulus Labill. by enzymatic mild acidolysis (EMAL). Holzforschung 62(1): 24-30.

Kim, K.H., Moon, S. J., Lee, S. M., Yeo, H. M., Choi, I. G., Choi, J. W. 2011. Characterization of Pyrolytic Lignin in Biooil Produced with Yellow Poplar (Liriodendron tulipifera). Journal of the Korean Wood Science and Technology 39(1): 86-94.

Kim, J. Y., Oh, S., Hwang, H., Moon, Y., Choi, J. W. 2013. Evaluation of primary thermal degradation feature of M. sacchariflorus after removing inorganic compounds using distilled water. Journal of the Korean Wood Science and Technology 41(4): 276-286.

Kim, J.-Y., Lee, J.H., Park, J., Kim, J.K., An, D., Song, I.K., Choi, J.W. 2015a. Catalytic pyrolysis of lignin over HZSM-5 catalysts: effect of various parameters on the production of aromatic hydrocarbon. Journal of Analytical and Applied Pyrolysis 114: 273-280.

Kim, J.Y., Lee, J.H., Park, J., Kim, J.K., An, D., Song, I.K., Choi, J.W. 2015b. Catalytic pyrolysis of lignin over HZSM-5 catalysts: Effect of various parameters on the production of aromatic hydrocarbon. Journal of Analytical and Applied Pyrolysis 114: 273-280.

Kim, K.H., Bai, X.L., Cady, S., Gable, P., Brown, R.C. 2015c. Quantitative Investigation of Free Radicals in Bio-Oil and their Potential Role in Condensed-Phase Polymerization. Chemsuschem 8(5): 894-900.

Kim, K.H., Kim, C.S. 2018. Recent Efforts to Prevent Undesirable Reactions From Fractionation to Depolymerization of Lignin: Toward Maximizing the Value From Lignin. Frontiers in Energy Research 6.

Kim, K.H., Eudes, A., Jeong, K., Yoo, C.G., Kim, C.S., Ragauskas, A.J. 2019. Integration of renewable deep eutectic solvents with engineered biomass to achieve a closed-loop biorefinery. Proceedings of the National Academy of Sciences of the United States of America 116(28): 13816-13824.

Mahon, E.L., Mansfield, S.D. 2019. Tailor-made trees: engineering lignin for ease of processing and tomorrow's bioeconomy. Current Opinion in Biotechnology 56: 147-155.

Ragauskas, A.J., Beckham, G.T., Biddy, M.J., Chandra, R., Chen, F., Davis, M.F., Davison, B.H., Dixon, R.A., Gilna, P., Keller, M., Langan, P., Naskar, A.K., Saddler, J.N., Tschaplinski, T.J., Tuskan, G.A., Wyman, C.E. 2014. Lignin Valorization: Improving Lignin Processing in the Biorefinery. Science 344(6185): 1246843.

Shi, J., Pattathil, S., Parthasarathi, R., Anderson, N.A., Kim, J.I., Venketachalam, S., Hahn, M.G., Chapple, C., Simmons, B.A., Singh, S. 2016. Impact of engineered lignin composition on biomass recalcitrance and ionic liquid pretreatment efficiency. Green Chemistry 18(18): 4884-4895.

Sibout, R., Eudes, A., Mouille, G., Pollet, B., Lapierre, C., Jouanin, L., Seguin, A. 2005. CINNAMYL ALCOHOL DEHYDROGENASE-C and -D are the primary genes involved in lignin biosynthesis in the floral stem of Arabidopsis. Plant Cell 17(7): 2059-2076.

Socha, A.M., Parthasarathi, R., Shi, J., Pattathil, S., Whyte, D., Bergeron, M., George, A., Tran, K., Stavila, V., Venkatachalam, S., Hahn, M.G., Simmons, B.A., Singh, S. 2014. Efficient biomass pretreatment using ionic liquids derived from lignin and hemicellulose. Proceedings of the National Academy of Sciences of the United States of America 111(35): E3587-E3595.

Yang, Q., Pan, X.J. 2016. Correlation Between Lignin Physicochemical Properties and Inhibition to Enzymatic Hydrolysis of Cellulose. Biotechnology and Bioengineering 113(6): 1213-1224.

Zhao, Q., Tobimatsu, Y., Zhou, R., Pattathil, S., Gallego-Giraldo, L., Fu, C., Jackson, L.A., Hahn, M.G., Kim, H., Chen, F. 2013. Loss of function of cinnamyl alcohol dehydrogenase 1 leads to unconventional lignin and a temperature-sensitive growth defect in Medicago truncatula. Proceedings of the National Academy of Sciences 110(33): 13660-13665.